Runaway electron losses enhanced by resonant magnetic perturbations

G. Papp 1,2), M. Drevlak 3), T. Fülöp 1), P. Helander 3) and G.I. Pokol 2)

1) Nuclear Engineering, Department of Applied Physics, Chalmers University of Technology, Association EURATOM-VR, Göteborg, Sweden
2) Department of Nuclear Techniques, Budapest University of Technology and Economics, Association EURATOM-HAS, Budapest, Hungary
3) Max-Planck-Institut für Plasmaphysik, Greifswald, Germany

e-mail contact of main author: papp@chalmers.se

Abstract. Disruptions in large tokamaks can lead to the generation of a relativistic runaway electron beam that may cause serious damage to the first wall. To suppress the runaway beam the application of resonant magnetic perturbations (RMP) has been suggested. In this work we investigate the effect of resonant magnetic perturbations on the confinement of runaway electrons by simulating their drift orbits in magnetostatic perturbed fields and calculating the transport and orbit losses for various initial energies and different magnetic perturbation configurations. In the simulations we use model configurations with existing (TEXTOR) and planned (ITER) RMP systems, and solve the relativistic, gyro-averaged drift equations for the runaway electrons including the electric field, radiation losses and collisions. The results indicate that runaway electrons are well confined in the core of the device, but the onset time of runaway losses closer to the edge is dependent on the magnetic perturbation level, which can thereby affect the maximum runaway current. Runaway electrons are rapidly lost from regions where the normalised perturbation amplitude $\delta B/B$ is larger than $\sim$0.1% in a properly chosen perturbation geometry. This applies to the region outside the radius corresponding to the normalised flux $\psi = 0.5$ in ITER, when the ELM mitigation coils are used at maximum current in their most favourable configuration.

1. Introduction

Disruptions in large tokamaks can lead to the generation of a relativistic runaway electron beam that may cause serious damage to the first wall. The avalanching effect increases the number of runaways exponentially, leading to runaway currents of several megaamperes in a large tokamak. The uncontrolled loss of such a high energy electron beam is intolerable and therefore the issue of how to avoid or mitigate the beam generation is of prime importance for ITER.

As a possible way to help suppressing the runaway beam the application of resonant magnetic perturbations (RMP) has been suggested. A large number of promising experiments [1–4] suggest that the application of RMP is capable of decreasing or even stopping the avalanching of runaways. However, the results were not uniformly positive in every tokamak [5]. The reason for the difference in the experimental success of suppressing runaways in various devices is not yet properly understood. The ITER ELM mitigation coils can, in principle, be used for runaway mitigation purposes. A reliable picture of how the runaway electrons are transported out of the plasma can only be obtained via three-dimensional numerical modelling. Earlier theoretical [6] and numerical [7] works suggested that runaway losses are greatly enhanced in the regions where the normalized perturbation amplitude is higher than $\delta B/B \simeq 10^{-3}$. This applies to the region outside the radius corresponding to the normalised toroidal flux $\psi \simeq 0.7 - 0.8$ in TEXTOR [8]

and $\psi \simeq 0.5$ in ITER [9].

In this work we investigate the effect of RMP on the confinement of runaway electrons by simulating their drift orbits in magnetostatic perturbed fields and calculating the transport and orbit losses for various initial energies and different magnetic perturbation configurations.

2. Modelling

We solve the relativistic, gyro-averaged equations of motion for the runaway electrons including the effect of synchrotron and Bremsstrahlung radiation with the ANTS (plasmA simulatioN with drifT and collisionS) code [8]. This code calculates the drift motion of particles in 3D fields and takes into account collisions with background (Maxwellian) particle distributions, using a full-f Monte Carlo approach with a collision operator that is valid for both non-relativistic and relativistic energies. We follow a test particle approach: independent test particles with given initial conditions for position $\mathbf{r}_0$ and velocity $\mathbf{v}_0$ are launched and their orbits are integrated in predefined 3D static magnetic structures. The particles are considered lost if they leave the computational zone, that is the original last closed flux surface (LCFS) of the device.

The 3D magnetic field is defined on a mesh in the entire domain of computation, and the integration of the particle orbits is carried out in Cartesian coordinates. This approach provides the greatest flexibility and facilitates a faithful treatment of magnetic fields with islands and ergodic zones, since the existence of magnetic surfaces is not required. If stellarator symmetry can be assumed, like in the case of TEXTOR, the memory demand of the calculations is reduced significantly. Results obtained in this coordinate system then can be transformed to flux coordinates for better visualization [9]. We have to note however, that the definition of the exact flux coordinate system in a 3D perturbed equilibrium is fairly complicated and is outside the scope of the present investigation.

2.1. TEXTOR

We first studied the runaway electron drift orbits in TEXTOR-like perturbed magnetostatic fields and evaluated the effect of RMP coils on runaway loss enhancement. The main reason for this choice is that it has been shown experimentally on TEXTOR that runaway losses can be enhanced by the application of RMP [3, 4]. At sufficiently high perturbation levels a reduction of the runaway current was observed. The variety of published experimental results at TEXTOR concerning RMP and runaways makes it possible to benchmark the numerical results.

The plasma parameters were chosen to be similar to the ones where the runaways were shown to be suppressed by resonant magnetic perturbations created by the Dynamic Ergodic Divertor (DED) [10] coils. The unperturbed magnetic equilibrium has been calculated by the VMEC [11] equilibrium code. The magnetic field perturbations are modelled to be similar to the ones produced by DED-coils on TEXTOR in the 6/2 DC operation mode [10], that has a 180° toroidal rotation symmetry, hence the generated perturbation has a lead toroidal mode number of $n = 2$. The coils create magnetic perturbations at the plasma periphery on the high field side of the torus that decay radially toward the inside of the plasma, as shown in figure 1a.

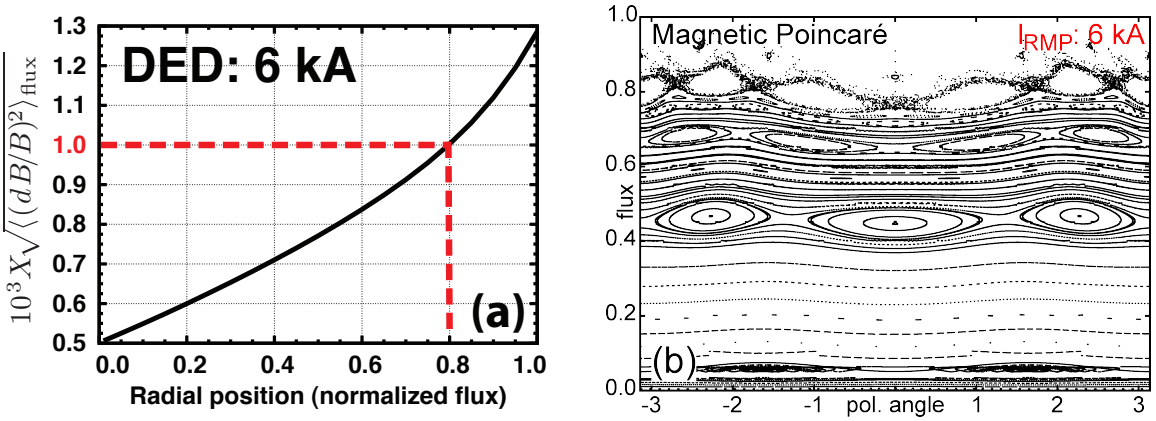

Figure 1: *6/2 DC configuration at $I_{\mathrm{DED}} = 6$ kA. (a) Radial dependence of the flux surface averaged $\sqrt{\langle(\delta B/B)^2\rangle}$. (b) Magnetic field structure in the perturbed equilibrium. The critical $\delta B/B \simeq 10^{-3}$ is reached at ψ=0.8, where significant ergodization is visible.*

We neglect the effect of shielding of magnetic field perturbations by plasma response currents. This approximation is expected to be valid in cold post-disruption plasmas. Including shielding of any strength would reduce the perturbation, thus our results should be interpreted as an upper limit on the actual losses. The maximal current available in the DED is limited at 7.5 kA due to technical reasons. Close to the upper limit, at 6 kA, the coils are capable of creating the $\delta B/B = 10^{-3}$ magnetic perturbation level that is predicted to be necessary for runaway suppression [6] up to the flux surface $\psi = 0.7 - 0.8$. The perturbed TEXTOR-like equilibrium for 6 kA DED current is illustrated in figure 1b. Clearly, the edge region becomes ergodic and particles outside the last intact magnetic surface are expected to leave the plasma rapidly.

The drift topology for high energy particles can significantly differ from the magnetic topology in both perturbed and unperturbed magnetic fields [12]. In principle, electrons can gain up to 20 MeV extra energy during a TEXTOR disruption [8]. Runaway electrons in the exess of 25 MeV have been reported on TEXTOR [3]. At such high energies there is a significant deviation from the magnetic topology. Therefore, we have introduced particle Poincaré plots (figure 2) that allow us to determine how the confinement changes with different particle energies and perturbation currents. The structure visible in figure 2d resembles the one shown in figure 1b: as expected, the drift topology of the low energy particles is fairly similar to the magnetic field structure. As expected, the effect of the DED decreases with increasing particle energy; at higher energies the edge stochastization and enhanced confinement volume shrinkage is less visible.

Even in the unperturbed case, the confinement volume shrinks as the particle population is shifted with increasing energy, as illustrated in figure 2. The drift orbits (in the unperturbed field) of the particles are circles that are displaced horizontally with respect to the flux surfaces, with a displacement that is proportional to the energy (for relativistic particles). Since the population is shifted, the outermost particles intersect the LCFS that causes a shrinkage of the effective confinement zone. This shrinkage of the confinement zone plays an important role at high particle energies regardless of the DED. However, high energy particles are kept confined within their new LCFS, hence the core runaways remain intact.

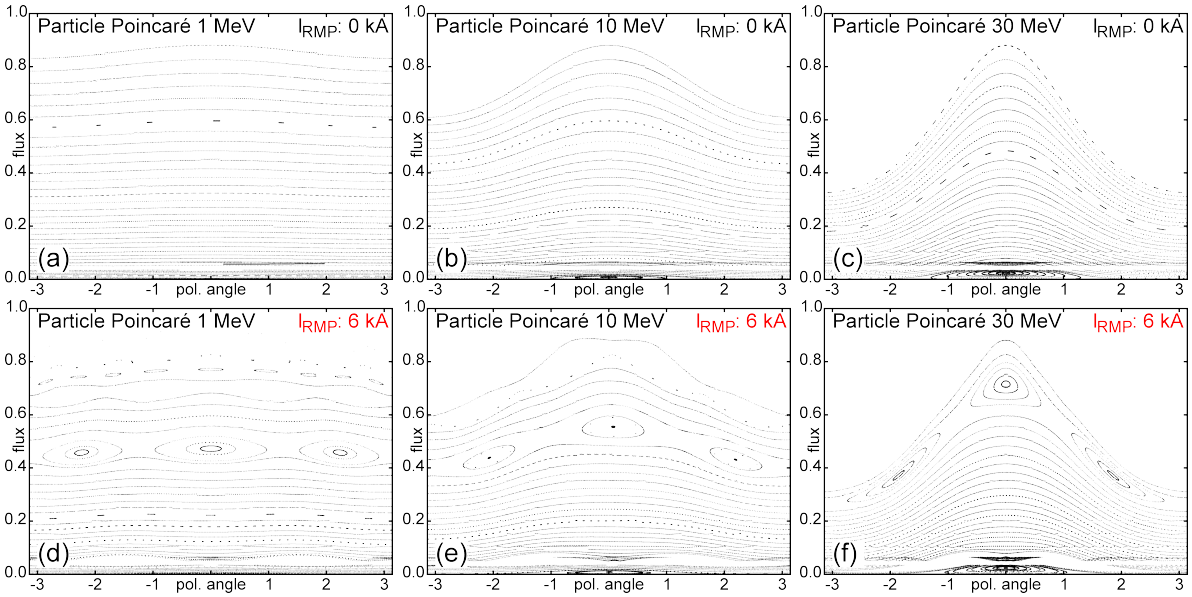

Figure 2: *Poincaré plots of the particle orbits, the particle energies are (a,d) 1, (b,e) 10 and (c,f) 30 MeV. Even without perturbation (a-c), the confinement volume shrinkage due to the energy gain is clearly observable. (d-f) Poincaré plots for* $I_{\mathrm{DED}} = 6$ kA. *Significant enhancement of the confinement volume shrinkage is only visible in the low-energy (d) case.*

2.2. ITER

The ITER simulations have been carried out for ITER scenario #2 (15 MA inductive burn) [13]. Inductive scenarios are expected to produce the largest and most energetic populations of runaway electrons. In the simulations a cold (10 eV [14]) post-disruption equilibrium is used. The cold equilibrium was calculated with VMEC, based on the plasma parameter profile shapes obtained by warm plasma simulations with the ASTRA code [13].

The time-dependent electric field accelerating the runaways was modelled in an ITER-like disruption scenario using a model for the coupled dynamics of the evolution of the radial profile of the current density (including the runaways) and the resistive diffusion of the electric field [15]. Particles can reach energies in excess of 100 MeV, but the avalanche runaway distribution will be dominated by $\mathcal{O}(10)$MeV particles. Here, just as with TEXTOR, we neglect the effect of shielding of magnetic field perturbations by plasma response currents. The perturbed magnetic field is obtained by superimposing the field from the ELM perturbation coils on the field of the unperturbed VMEC solution.

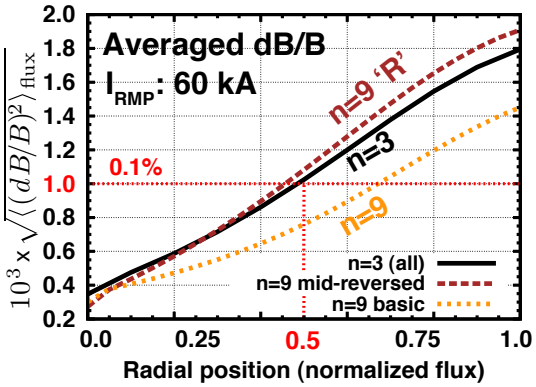

Figure 3: *Radial dependence of the flux surface average* $\sqrt{\langle(\delta B/B)^2\rangle}$ *for* $I_{\mathrm{RMP}} =$ 60 kA *in* $n = 9$ *and* $n = 3$ *operational modes.*

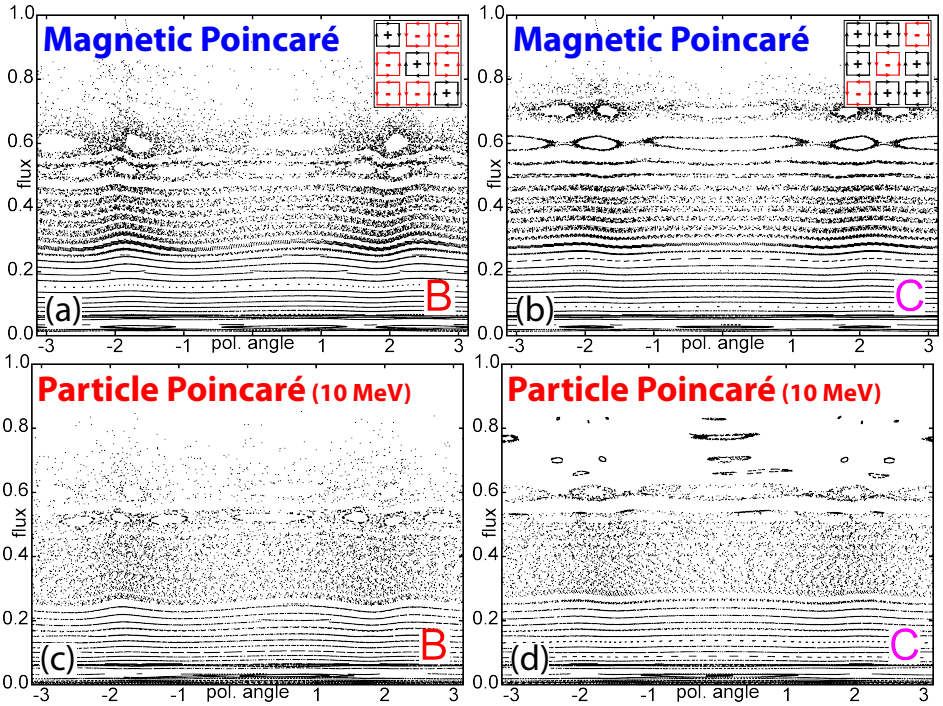

Figure 4: *Magnetic (a-b) and particle (c-d) Poincaré plots visualize the difference between configurations "B" and "C". Sketch of the current configuration is shown in the corners of (a-b).*

The ELM perturbation coil-set consists of 9×3 quasi-rectangular coils at the low field side, that allows for a wide variety of possible current configurations [9]. Two $n = 3$ current configurations, marked with "B" and "C" in ref. [9], are presented in this paper. The configurations have identical perturbation strength (see figure 3), but due to the current flowing in different directions in the various coils – as indicated in the by the pictograms in the top right corner of the figures – these can give rise to quite different magnetic structures, and hence, different loss enhancement.

Figure 4 shows magnetic- and particle Poincaré plots to visualize the different effect of the most successful "B" and the least successful "C" configuration. In the case of "B", a wide ergodic zone forms at the edge of the plasma starting at $\psi \simeq 0.5$, that enhances radial transport of particles. In the case of "C", edge islands trap and confine the particles for longer times, leading to only a slight transport increase.

3. Runaway loss enhancement

3.1. TEXTOR

The DED can significantly influence only the low-energy ($\simeq 1$ MeV) particles closer to the boundary (figure 2d). For these particles the onset time of the losses is dependent on the amplitude of the magnetic perturbation, and this can affect the maximal runaway current. In the unperturbed case, as is visible in figure 5, losses for particles launched at $\psi_0 = 0.7$ start at $\simeq 2.8$ ms, while with DED, the losses start at $\simeq 2.2$ ms. The time dependence of the following losses – the runaway current damping rate – is insensitive to the magnetic perturbation level. This and its experimentally measured value is consistent

with our simulations. Synchrotron radiation emission did not contribute much to the losses, mainly due to the fact that the time-scale of these losses is much longer than the runaway loss time.

The simulations described did not explain the loss of core runaways as was observed in the experiments. However, according to ref. [16], the loss of the core runaways is enhanced by MHD perturbations onset by the disruption. These perturbations can expel a significant amount of runaways from the core to the edge in a small scale device like TEXTOR. The RMP can enhance the losses of the runaways once those are close to the edge. This could explain the observed enhancement of runaway losses due to the RMP in small tokamaks. For JET, the MHD perturbations are not sufficient to expel the particles from the core, which could be the reason why RMP does not seem to be effective in JET [5].

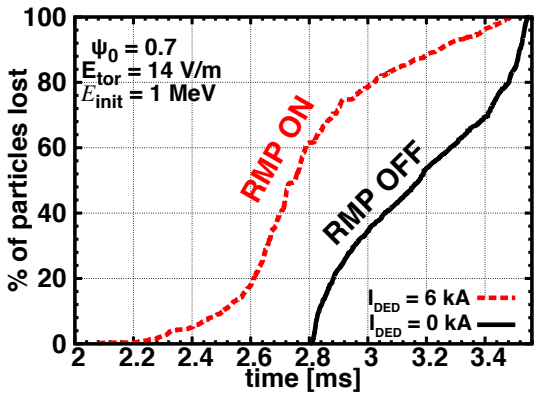

Figure 5: *Time dependence of particle losses for 1 MeV particles, launched at $\psi_0 = 0.7$. RMP decreases the onset time of the losses by ∼20%.*

3.2. ITER

Even in the unperturbed case, the confinement volume shrinks as the particle population is shifted towards the Low Field Side (LFS) with increasing energy. Confinement volume shrinkage for 10 MeV particles is visualized in figure 6a for cases with and without RMP. As expected, at lower energies such as 10 MeV, the particles are mostly confined in the unperturbed case, and in the least effective configuration "C". In the case of "B", the confinement volume shrinkage is largely increased, up to 50%. Therefore, in the following we will study the losses caused by the "B" perturbation configuration. For higher energies, such as 100 MeV, RMP is less effective: confinement volume shrinkage can be up to 50% without perturbation, further increased until 60% in case "B".

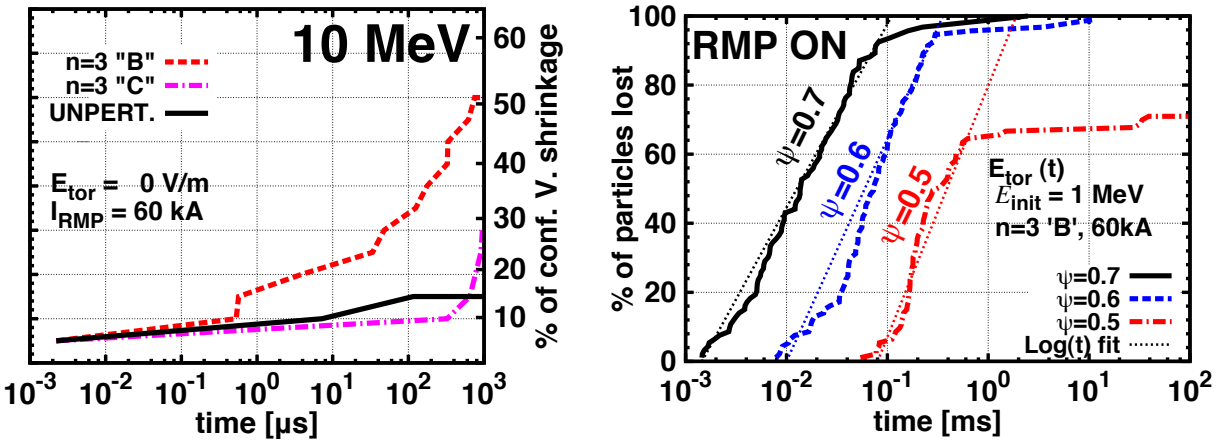

Figure 6: *(a) Confinement volume shrinkage for two different $n = 3$ perturbations for 10 MeV particles. (b) Particles losses with RMP.*

If we launch 1 MeV particles on a flux surface that is within the confinement zone but will be outside it at large energies e.g. $\psi = 0.7$, we observe particle losses even without perturbation. This is caused solely by the high energy that the particles reach during the disruption. Without the RMP, particle losses from $\psi = 0.7$ start around 10 ms and finish by 11 ms.

In the perturbed case the ergodic zone arising at the edge causes losses several orders of magnitude faster than in the unperturbed case. As shown on figure 6b, particles launched at $\psi = 0.7$ start to get lost already after 1 μs, and losses continue with logarithmic temporal dependence until ~ 0.1 ms (note the logarithmic time axis on the figure). At around 0.1 ms already 95% of the particles are lost, but the remaining 5% takes up to 2-3 ms to get lost. Similar dynamics is observable if the particles are launched at the flux-surface $\psi = 0.6$. The particle losses start an order of magnitude later at 10 μs, and dynamics of the losses is the same: logarithmic losses up to ~ 0.2 ms, where around 95% of the particles are lost, followed by a longer period during what the remaining particles are also lost within 10 ms. If we go one more $\Delta\psi = 0.1$ step further in, the losses start again 10 times later at 100 μs, and the logarithmic dependence is the same. In this case not all the particles will be lost, since the high energy LCFS is in the vicinity of the $\psi = 0.5$ surface. Particles launched further in, e.g. at $\psi \lesssim 0.5$ will not get lost even with strong RMP.

The choice of perturbation configuration not only alters the final confinement volume shrinkage, but the loss dynamics can be varied by orders of magnitudes as well. We have to emphasize that the relative perturbation magnitude and the symmetry (toroidal modenumber) is the same in all of these cases, only the alignment with respect to the unperturbed field lines is different. This shows the chaotic nature of magnetic field perturbations and the importance of numerical estimates on the effectiveness of possible configurations before the actual realization of the RMP system.

The logarithmic loss dynamics show that most of the particles are lost during the early phases of the losses, which seems to be favourable from the avalanche generation point of view. Also, the particles lost due to RMP have low energy, while the losses caused by the shrinkage of the confinement zone result in lost particles in the 100 MeV energy range. Thus, RMP not only increases the amount of the particles lost outside ψ=0.5, it might also significantly weaken the avalanche generation in that region and result in lost particles at several orders of magnitude lower energies. All of these results seem to be beneficial from the runaway electron suppression point of view. However, losing fast electrons from the edge may lead to a larger inductive field in the centre of the plasma, making the avalanche stronger there. Therefore, quantitative conclusions about the magnitude of the total runaway current can only be drawn from simulations where both the evolution of the electric field and losses due to RMP are included self-consistently. This could be achieved e.g. by the ARENA code [17, 18], using the results presented in this paper as input, possibly in a form of radial transport coefficients and/or time-dependent losses at the edge.

4. Summary

High-energy population of runaway electrons that can form in disruptions pose a serious threat to reactor-scale tokamaks like ITER, and the runaway generation has to be mitigated for safe operation. One possible option for runaway removal is to artificially generate ergodic zones by external resonant magnetic perturbation (RMP). The aim of this ergodisation is to remove runaway electrons from the plasma before they reach high energy. The experimental results are inconclusive, showing success on several tokamaks but not on others. Numerical analysis is necessary to better understand the phenomenon.

After developing a suitable numerical method we first aimed at understanding the experimental results measured on the TEXTOR tokamak. We found that runaway electrons in the core of the plasma are likely to be well confined. For low-energy ($\simeq 1$ MeV) particles closer to the boundary, where the $\delta B/B \gtrsim 10^{-3}$ criterion is met, the onset time of the losses is dependent on the amplitude of the magnetic perturbation, and this should affect the maximal runaway current. The runaway current damping rate is insensitive to the magnetic perturbation level, and its experimentally measured value is consistent with our simulations. We also found that a significant loss of runaways occurs independently of the RMP, as a result of the confinement volume shrinkage at larger energies. We surmise that the experimental success of RMP on smaller devices can be understood by taking more complex effects such as, e.g., MHD perturbations into account.

We also investigated the efficacy of the proposed ITER RMP system for runaway mitigation. As expected, we found that runaways in the core ($\psi \lesssim 0.6$) are well confined. According to our simulation results, in a properly chosen perturbation geometry runaways are rapidly lost if $\delta B/B \gtrsim 10^{-3}$, which corresponds to the region outside the normalised flux $\psi = 0.6$.

The losses are partly caused by the confinement volume shrinkage caused by the energy gain, and partly by the increased radial transport in the stochastic region induced by the RMP. We performed simulations for several perturbation configurations and concluded that runaway losses are quite sensitive to the perturbation configuration. We identified one of the possible $n = 3$ perturbations to be the most efficient in this respect. The results indicate that the presence of RMP not only increases the number of lost particles, but may also influence the avalanche generation at the edge, since it leads to earlier losses of particles with lower energies. The actual effect of the RMP on the global runaway electron population and dynamics can only be calculated with more complex simulations that take into account the electric field dynamics self-consistently. This could be achieved, e.g., by the ARENA code [17, 18], using the results presented in this paper as input.

Acknowledgments

This work was funded by the European Communities under Association Contract between EURATOM, *Vetenskapsrådet*, HAS and Germany. The views and opinions expressed herein do not necessarily reflect those of the European Commission.

References

[1] P. Ghendrih et al. Plasma Physics and Controlled Fusion, **38** (10):1653 (1996).
[2] R. Yoshino et al. Nuclear Fusion, **40** (7):1293 (2000).
[3] M. Lehnen et al. Phys. Rev. Lett., **100** (25):255003 (2008).
[4] M. Lehnen et al. Journal of Nuclear Materials, **390-391**:740 (2009).
[5] V. Riccardo et al. Plasma Physics and Controlled Fusion, **52** (12):124018 (2010).
[6] P. Helander et al. Physics of Plasmas, **7** (10):4106 (2000).
[7] T. Fehér et al. Plasma Physics and Controlled Fusion, **53** (3):035014 (2011).
[8] G. Papp et al. Nuclear Fusion, **51** (4):043004 (2011).
[9] G. Papp et al. Plasma Physics and Controlled Fusion, **53** (9):095004 (2011).
[10] K. Finken et al. *The structure of magnetic field in the TEXTOR-DED*. Grafische Medien, Forschungszentrum Jülich GmbH, Jülich (2005).
[11] S. P. Hirshman et al. Computer Physics Communications, **43** (1):143 (1986).
[12] X. Guan et al. Physics of Plasmas, **17** (9):092502 (2010).
[13] A. Polevoi. Tech. Rep. 22KZK3, ITER Documentation System (IDM) (2002).
[14] T. Hender et al. Nuclear Fusion, **47** (6):S128 (2007).
[15] H. M. Smith et al. Plasma Physics and Controlled Fusion, **51** (12):124008 (2009).
[16] V. Izzo et al. Nuclear Fusion, **51** (6):063032 (2011).
[17] L. G. Eriksson et al. Computer Physics Communications, **154** (3):175 (2003).
[18] L.-G. Eriksson et al. Phys. Rev. Lett., **92** (20):205004 (2004).